IOP Publishing and International Atomic Energy Agency Nuclear Fusion
Nucl. Fusion **47** (2007) 825–832 doi:10.1088/0029-5515/47/8/013

Evidence for anomalous effects on the current evolution in the tokamak hybrid operating scenarios

T.A. Casper[1], R.J. Jayakumar[1], S.L. Allen[1], C.T. Holcomb[1], L.L. LoDestro[1], M.A. Makowski[1], L.D. Pearlstein[1], H.L. Berk[2], C.M. Greenfield[3], T.C. Luce[3], C.C. Petty[3], P.A. Politzer[3] and M.R. Wade[3]

[1] Lawrence Livermore National Laboratory, PO Box 808, Livermore, CA 94550, USA
[2] Institute for Fusion Studies, The University of Texas, Austin, Texas, USA
[3] General Atomics, PO Box 85608, San Diego, CA 92186-5608, USA

E-mail: casper1@llnl.gov

Received 11 January 2007, accepted for publication 17 May 2007
Published 23 July 2007
Online at stacks.iop.org/NF/47/825

Abstract
Alternatives to the usual picture of advanced tokamak (AT) discharges are those that form when anomalous thermal conductivity and/or resistivity alter plasma current and pressure profiles to achieve stationary characteristics through self-organizing mechanisms where a measure of desired AT features is maintained without external current-profile control. Regimes exhibiting these characteristics are those where the safety factor (q) evolves to a stationary profile with the on-axis and minimum $q \sim 1$. Operating scenarios with fusion performance exceeding H-mode at the same plasma current and where the inductively driven current density achieves a stationary configuration with either small or nonexisting sawteeth should enhance the performance of ITER and future burning plasma experiments. We present simulation results of anomalous current-profile formation and evolution using theory-based hyper-resistive models. These simulations are stimulated by experimental observations with which we compare and contrast the simulated evolution. We find that the hyper-resistivity is sufficiently strong to modify the current-profile evolution to achieve conditions consistent with experimental observations. Modelling these anomalous effects is important for developing a capability to scale current experiments to future burning plasmas.

PACS numbers: 52.25.Fi, 52.25.Xz, 52.35.Py, 52.55.Fa, 52.65.Kj

(Some figures in this article are in colour only in the electronic version)

1. Introduction

Experiments worldwide have discovered inductively driven operating configurations with moderately high performance where the q-profile becomes stationary, that is, the time-averaged shape does not change significantly and discharge parameters achieve quasi-steady values. In these discharges, the q-profile becomes relatively flat with, on average, $q_{\min} \approx q_0 \approx 1$, where $q_{\min}$ is the minimum q value and q_0 is the value at the magnetic axis. As is evidenced by the nontime-varying trend in pitch angle data from motional Stark effect (MSE) measurements, these stationary conditions have been observed in several experiments in two distinctly different operating regimes, the hybrid [1–4] and quiescent double barrier (QDB) [5] modes. We address hybrid conditions here and present evidence that anomalous current diffusion can alter the q-profile evolution consistent with observations on the DIII-D tokamak. We use modelling of discharges to compare and contrast with these experimental observations.

In hybrid scenarios, while the usual feedback control of density and power is employed, a key ingredient is the ability to passively sustain a stationary current-density profile with safety factor at the magnetic axis, q_0, close to unity and, therefore, with minimal or no sawteeth over several current diffusion times. This permits operation with higher performance and normalized $\beta_N = \beta/(I/aB_T)$ closer to the no-wall limit. In DIII-D hybrid discharges, stationarity appears to be closely linked to the presence of continuous $n = 2$ or $n = 3$ neoclassical tearing mode (NTM) activity [6]. Without these relatively benign $n > 1$ NTM fluctuations, discharges

typically will either develop a strong $n = 1$ NTM and disrupt if the internal magnetic fluctuations interact with external field errors to slow the rotation (mode locking) or relax to a standard sawtoothing discharge with lower confinement. We introduce a new hyper-resistive (HR) [7] term in Ohm's law to model the evolution of the current density profile subject to NTM activity and compare the anomalous evolution of these hybrid discharges with a modelled evolution to assess these effects. These comparisons provide estimates of how well the HR modelled evolution describes the experimental conditions. Experimental and theoretical efforts are underway to find the precise mechanism by which these NTMs interact with other modes to maintain $q_0 \sim 1$ [8].

The ability to experimentally enter this DIII-D hybrid regime depends sensitively on the plasma startup conditions that must produce current density and pressure profiles consistent with the excitation of a finite-island-width NTM. Failure to excite such a mode or, equivalently, stabilization of the NTM present precludes hybrid-mode operation. Subtle modifications to experimental conditions can thus alter the discharge evolution. We are exploring by means of numerical simulations such subtleties in the evolution of the current profile that reflect possible changes in the experiment. Our intention is to demonstrate the degree to which current diffusion is capable of altering the early evolution of the q-profile and of modelling the phenomena necessary to enter and sustain the stationary evolution late in time with $q_0 \sim 1$.

2. HR model for current diffusion due to NTMs in the CORSICA code

In the CORSICA transport code [9], we have modified our Ohm's law implementation with the addition of the new HR (current diffusion) term to simulate the effects of neoclassical islands using a model by Berk, Fowler, LoDestro and Pearlstein (BFLP) [10]. This will be used in combination with an existing HR model due to Ward and Jardin (WJ) [11] to simulate the plasma evolution. This NTM island physics model is a relatively new addition and we outline its implementation here. The HR effects are generated by time-independent, field-line entanglement according to the Rechester–Rosenbluth [12] approach. The additional feature is a HR response due to the turbulence. We start with the drift-kinetic equation for electrons and perform a quasi-linear analysis [10] to obtain

$$\frac{\partial f_0}{\partial t} + v_\parallel \frac{\partial f_0}{\partial s} = C\,(f_0) - \frac{v_\parallel}{B}\nabla \cdot \left(\tilde{B} \left| \tilde{B} \cdot \nabla \psi \right| \frac{v_\parallel}{B} \cdot \frac{\tilde{\nu}}{\tilde{\nu}^2 + k_\parallel^2 v_{\rm th}^2} \frac{\partial f_0}{\partial \psi} \right) \equiv C\ (f_0) + D(f_0). \tag{1}$$

The first term on the right-hand side is the usual Fokker–Planck operator (C) while the second term (D) represents Rechester–Rosenbluth transport where ψ is the poloidal flux and $\tilde{\nu}$ is the effective collision frequency that depends upon the collisionality regime within the island. Ohm's law can be written as

$$E + \frac{v}{c} \times B = \frac{m}{ne} \int v_\parallel \, {\rm d}^3 v [C(f_0) + D(f_0)], \tag{2}$$

and, using this in Faraday's law with the standard averages, the magnetic flux diffusion equation,

$$\frac{\partial \psi}{\partial t} = \eta \frac{\langle J \cdot B \rangle}{\langle B \cdot \nabla \varphi \rangle},$$

$$\text{or, with } \langle \cdots \rangle = \oint \frac{{\rm d}l}{B} \cdots \Big/ \oint \frac{{\rm d}l}{B},$$

$$\frac{\langle B \cdot E \rangle}{\langle B \cdot \nabla \varphi \rangle} = \frac{\partial \psi}{\partial t} = \eta \frac{\langle J \cdot B \rangle}{\langle B \cdot \nabla \varphi \rangle} - \frac{1}{2\pi q} \frac{\partial}{\partial \psi} \oint \frac{{\rm d}l}{B} \times \frac{m}{ne^2} |\tilde{B} \cdot \nabla \psi|^2 \left\langle \frac{\tilde{\nu} v_{\rm th}^2}{\tilde{\nu}^2 + (k_{||} v_{\rm th})^2} \right\rangle \frac{\partial}{\partial \psi} \frac{J_{||}}{B}, \tag{3}$$

is obtained. Note that liberties have been taken to move terms through the operators so as to preserve helicity conservation. The first term on the right-hand side of equation (3) is the usual flux diffusion and the new term is the current diffusion. When averaging is performed, it is assumed that these terms are functions of density, n, and temperature, T. We assume that n is constant over an island.

All that remains is to determine the value of $\tilde{B} \sim w^2$ for w the island width. For this, we turn to the modified Rutherford equation [13, 14]:

$$\partial w/\partial t = 1.22\, \eta/\mu_0 [\Delta' + (D_{\rm R}/w) + D_{\rm neo}\, w/(w^2 + \bar{w}^2)], \tag{4}$$

where Δ' is the cylindrical tearing mode criteria, $D_{\rm R}$ the resistive interchange term [15] and $D_{\rm neo}$ the neoclassical island drive and $\bar{w}$ is a threshold in the neoclassical island equation. We do not include the polarization threshold term. Our purpose is to evaluate the impact of hyper-resistivity on the current and q-profile to explore the possibility that current diffusion is responsible for altering the evolution of q. In principle, this theory contains no adjustable parameters. In practice, we can adjust the neoclassical drive of order unity to keep the island size representative of that observed in the experiment. The use of cylindrical approximations to obtain Δ' for shaped tokamaks such as DIII-D is likely to lead to uncertainties of this order. We obtain the total HR coefficient by combining the models present. In the case of multiple NTM modes, the HR-coefficient for the BLFP model can be obtained by summing over the assumed non-interacting modes (mode–mode coupling is not included). At each time step in our simulations of the plasma evolution, we evaluate the total HR-coefficient and simultaneously solve for the new equilibrium with transport thus allowing the multiple modes and HR-models to interact as the equilibrium changes.

3. Hyper-resistive modelling of hybrid mode current-profile evolution

Using HR models in the CORSICA transport code, we explore the extent to which the observed current-profile evolution is consistent with modifications due to the presence of fluctuations driving diffusion of the local current density. We concentrate on a representative DIII-D hybrid-mode discharge, shot 117755, with parameters shown in figure 1 and a toroidal magnetic field of $B_{\rm T} = 1.7\,{\rm T}$, $\beta_{\rm N} = 2.7$ and confinement factor $H_{\rm L89} = 2.5$, the ITER89-P L-mode energy confinement enhancement factor. Some characteristics of this discharge were previously explored [16] using an *ad hoc* conductivity-flattening model to demonstrate the possibility of dynamo-like behaviour. Here, we expand on these simulations with a combination of HR models active over different regions.

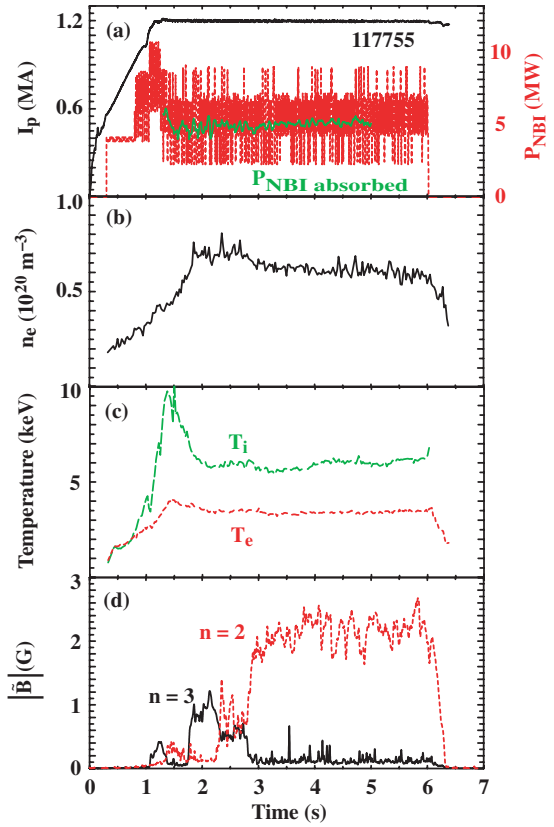

Figure 1. DIII-D hybrid shot 117755 experimental parameters: (*a*) plasma current and injected neutral-beam power under β_N-feedback control, (*b*) electron density, (*c*) electron and ion temperatures and (*d*) edge $n = 2, 3$ fluctuation amplitudes. Also shown in (*a*) is the simulated neutral-beam power computed in the CORSICA simulations.

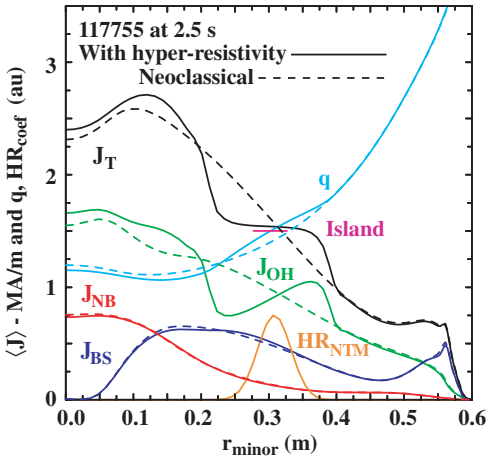

Figure 2. Flux-averaged current densities $\langle J\rangle$, q, and normalized HR coefficient at 2.5 s showing current diffusion due to the BFLP model flattening the J_T profile at the island and modifying the q profile evolution as compared with the neoclassical simulation. By $\langle J_k\rangle$, we mean $\langle J_k \cdot B\rangle/\langle B_T/R\rangle$ for $\langle\cdot\cdot\rangle$ indicating the flux-surface average.

In these simulations that use the BFLP model, we turn on a particular island based on experimental observations, figure 1(*d*). The island width and stability are determined from the modified Rutherford island evolution equation. Use of the modified Rutherford equation to predict the NTM island parameters has been experimentally verified and validated in NTM island stabilization experiments [14]. The island widths calculated in these simulations are comparable to those obtained in analysis of these experimental conditions. The BFLP model produces a localized HR coefficient that alters the current density and q profiles near the island location. We note that this current diffusion in the simulations is present in addition to the normal flux diffusion associated with peaking of the Ohmic current near the magnetic axis. In these simulations, we use spline fits to experimental measurements of the electron and impurity density and electron and ion temperature at 25 ms time intervals. Since numerical convergence of the HR computation in Ohm's law solutions requires advancement of the equilibrium at time intervals shorter than that available from the data, we interpolate over time between the available measurements. The noninductive current drive sources also simulated are the bootstrap current density (J_{BS}) from NCLASS [17] and the neutral-beam current (J_{NB}) using Monte Carlo deposition including the influence of the fast-ion drift orbits [18]. The total current (J_T) and Ohmic current (J_{OH}) densities are determined from competition between current and flux diffusion. We show the flux-surface-averaged current densities, $\langle J_k\rangle = \langle J_k \cdot B\rangle/\langle B_T R\rangle$ for current component k, and the resulting q-profile in figure 2 at 2.5 s during the time the overall q-profile is dropping due to normal flux diffusion inward responding to the Ohmic drive. We also show the normalized hyper-resistive coefficient resulting from the BFLP/NTM model to indicate regions where hyper-resistivity is active. In figure 3 we show the evolution of the neoclassical and Δ' stability terms in the modified Rutherford equation obtained in this simulation along with the calculated island location and width. Hyper-resistivity due to the NTM activity in the BLFP model is continuously active as indicated by the profile evolution in figure 4. Its cumulative effect is to continuously alter the evolution of the q profile. During the early evolution, the WJ model is inactive (HR-coefficient remains zero) since q is greater than 1. In figure 5, we show simulation q-profile contours modified by hyper-resistivity and the location of the predicted island evolution for shot 117755. The jump in the island parameters at 2.3 s is the time where we switch from an (m, n)-mode number of (5, 3) to a (3, 2)-mode in the simulations. This change in mode number is motivated by the shift in dominant mode numbers present in the experimental data as indicated in figure 1(*d*). The island size grows initially but saturates in width as a balance between the stabilizing Δ' and destabilizing neoclassical contributions is reached. In preliminary simulations with both modes simultaneously present (and interacting through changes to the equilibrium), after a short period of rapid change in the equilibria, a dominant mode survived and the sub-dominant mode rapidly stabilized (zero width) for these experimental conditions. This is not unlike the emergence of a dominant mode as shown in figure 1(*d*) except that the experimental time scale for change is much slower. As we have not yet explored these interactions that must be calculated on a finer time scale, we chose to use only a single dominant mode for these transport-time-scale simulations.

We show in figure 6 a comparison of the simulated temporal evolution of q_0, q_{min} and $r_{q\,min}$ (radius of q_{min})

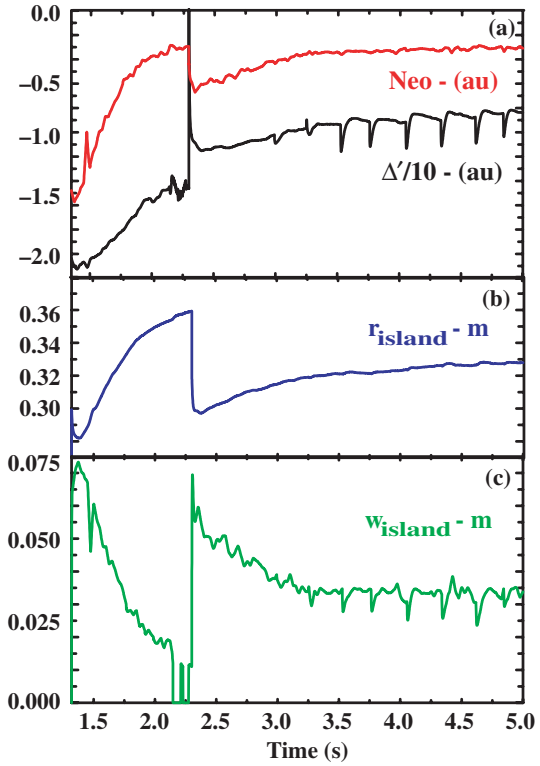

Figure 3. Stability terms in the modified Rutherford equation where in (*a*) 'Neo' is the destabilizing neoclassical term and Δ' is stabilizing and the calculated island (*b*) location and (*c*) width.

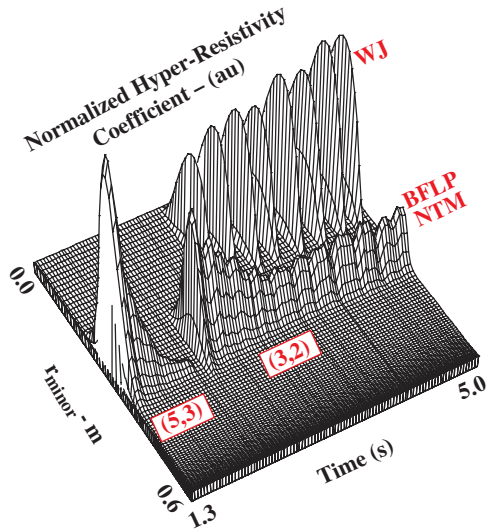

Figure 4. Normalized profiles of the HR coefficient for the two HR-models present in the simulation. The continuous HR-coefficient due to NTMs and the BFLP model is near $r \sim 0.3$ m with the transient effects due to WJ near the magnetic axis. Data in these regions are normalized separately to emphasize the nature and region of HR-activity for the two models.

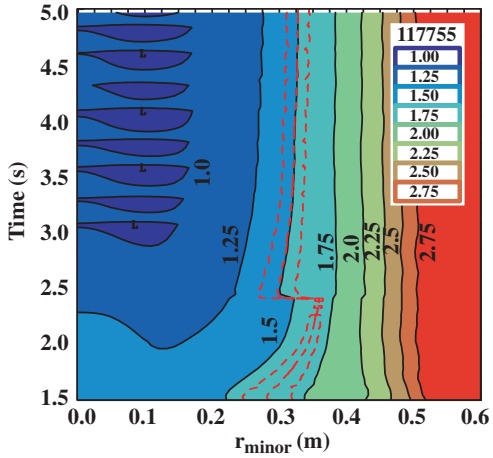

Figure 5. Evolution of q-profile contours computed using the HR models for 117755. The NTM island (dashed) evolution, $R_{\rm island} \pm W_{\rm island}/2$. A (5, 3)-mode is active from 1.55 to 2.3 s when we switched to a (3, 2)-mode. The structure inside $r_{\rm minor} = 0.15$ m is due to the WJ HR model transiently adjusting q_0 late in time.

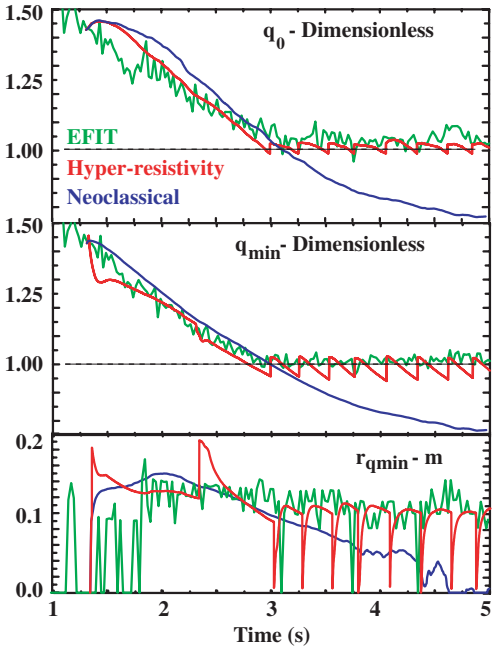

Figure 6. Consistency of q_0, $q_{\rm min}$ and $r_{q\,\rm min}$ evolution among HR-simulations, MSE-constrained EFIT and the comparison with a neoclassical evolution. The q profile responds to the change in mode from (5, 3) to (3, 2) at 2.3 s. The quasi-constant q is due to a combination of WJ limited by BFLP and flux diffusion rebuilding the current at the axis.

obtained in CORSICA simulations with and without hyper-resistivity with those from analysis of experimental data using a sequence of MSE-constrained EFIT solutions. We note that the q-profile (e.g. figure 2) well inside the island is relatively flat so q_0 and $q_{\rm min}$ are quite similar in magnitude. The time-dependent simulation using these HR models is in quantitatively better agreement with the experimentally fitted q_0, $q_{\rm min}$ and $r_{q\,\rm min}$ as compared with simulated evolution using only the neoclassical resistivity without the HR effects (neoclassical evolution). These parameters provide sensitive indicators of the effect of hyper-resistivity on the shape of the profile evolution. The pronounced changes are a direct result of the current diffusion resulting from the HR model. In particular, we note that the neoclassical evolution of q_0 and $r_{q\,\rm min}$ differ considerably from the HR result indicating a difference in the local shape of

the q profile. The relative insensitivity of $q_{\min}$ before the stationary phase comes in part from the fact that it depends on the integrated current density out to a given radius and the integrated current does not vary significantly under the effects of the highly localized current diffusion. However, the location of the $r_{q\,\min}$ is dependent on the localized perturbation in the current density as is indicated by the $J_{\rm OH}$ and $J_{\rm T}$ profiles shown in figure 2. The large excursion in $r_{q\,\min}$ for the HR-simulation at 2.3 s is a result of the instantaneous switch between the two NTMs. This switch in mode number instantaneously moves the resonant q location inwards (from $q = 1.67$ to 1.5) and results in rapid growth of the new island that changes the local shape of the q profile, e.g. $r_{q\,\min}$, as the island parameters readjust and saturate. The values of q_0 and $q_{\min}$ change much less dramatically as they depend on the more slowly changing current profile. In the experiment there is a more gradual transition from the (5, 3) to the (3, 2) mode and an interval where they are both active as indicated in figure 1(d) and thus, the EFIT $r_{q\,\min}$ remains more constant with time as the equilibrium evolves more slowly.

For a direct comparison with the experiment, we show the temporal MSE pitch angle measurements [19] and those from a synthetic MSE diagnostic inside CORSICA [20] in figure 7(a) for a channel near the magnetic axis. This shows good time-dependent agreement between the simulated and directly measured pitch angle data indicating that the simulated evolution using hyper-resistivity with a single active mode is in substantial agreement with the (unprocessed) experimental observations. We also show the simulated MSE data for the neoclassical evolution without hyper-resistivity. While for the most part these simulated data also remain within one standard deviation of the average MSE data, the temporal evolution is not as consistent with the measurements as is the HR evolution. In particular, the HR simulation tends to approach the measurements at the mode transitions. The rapid change in the synthetic measurement is a result of the instantaneous transition from the (5, 3)-mode to the (3, 2)-mode in the simulation. This results in a rapid modification of the current density near the island location that gives rise to the change in pitch angle shown as the (3, 2) NTM island grows and saturates in size. For example, at $t = 2.3$ s when we switch to the (3, 2)-mode, the simulated q_0 and $q_{\min}$ tend to better align with the measurements. This is similarly true for the transition to a stationary evolution at $t = 3$ s that we will discuss in the following section. What we infer is that the hyper-resistivity can provide a subtle but important modification to the current density and q-profile evolution as observed in experiments. In figure 7(b), we also show a comparison between the profiles of the synthetic diagnostic and the MSE data averaged over the beam-on time intervals at $t = 2$ s. We find the agreement to be quite respectable, particularly towards the inside of the discharge, e.g. $R < 2$ m. The discrepancy in the region of the NTM island indicates that fine-scale details of its effect on current diffusion may be slightly different than predicted by the HR model using a single predicted island location and size. Alternatively, we have included only the diamagnetic term in the radial electric field contribution to the synthetic MSE data whereas there can be a sizeable perturbation in the measurements due to toroidal rotation. At large radii (outside the island location) where the 'radial' and 'edge' arrays view

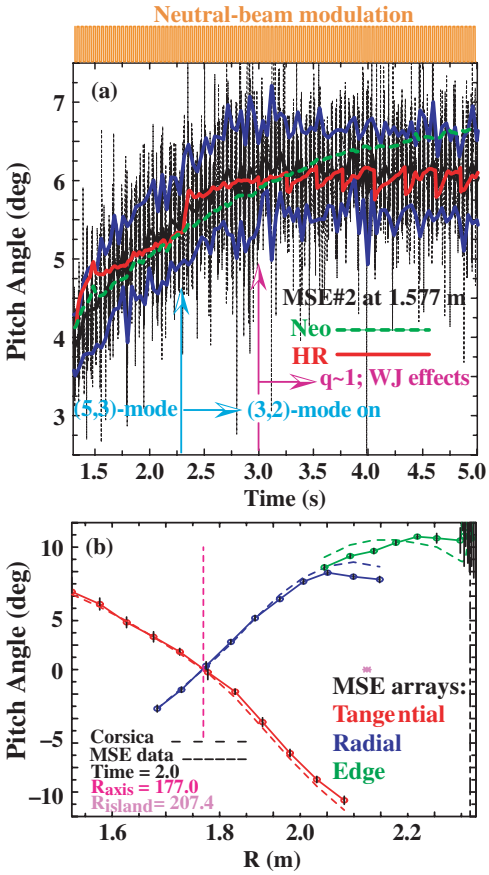

Figure 7. MSE pitch angles ($B_{\rm P}/B_{\rm T}$): (a) measured data (dotted), ⟨MSE⟩-averaged over the modulated 20 ms beam-on times (modulated at 50% duty cycle for background noise subtraction of MSE data), ⟨MSE⟩± one standard deviation and the simulated MSE data at $R = 1.577$ m for the HR (solid) and for the neoclassical (dashed) simulated evolution and (b) comparison of simulated and average measured MSE data over the plasma cross-section at $t = 2$ s.

the plasma, the agreement between simulated and real data is not as good as in the core. In this region, the radial MSE array suffers from a lack of radial resolution and we hypothesize that this is the difference between the simulated and real data. In the edge, the discrepancy is likely due to the experimental profile fits and/or the sizeable edge radial electric field that is located outside the island HR region. In this region, the current profile includes the local peak in the bootstrap current due to the pedestal gradients. In comparisons with the lithium ion beam measurements [21], we have found better agreement between the synthetic diagnostic and the measured edge magnetic field in other H-mode discharge comparisons.

4. The quasi-stationary evolution

We conclude that, during the time q is decreasing and the q-profile is relaxing to a stationary state, predictions of an anomalous current diffusion using the HR model with a single NTM island are consistent with the observed evolution inside the island location. During the quasi-steady conditions, however, simulations with a single NTM resonant near the mid-radius using the BFLP model result in localized current diffusion that is not sufficiently strong to explain the flattening

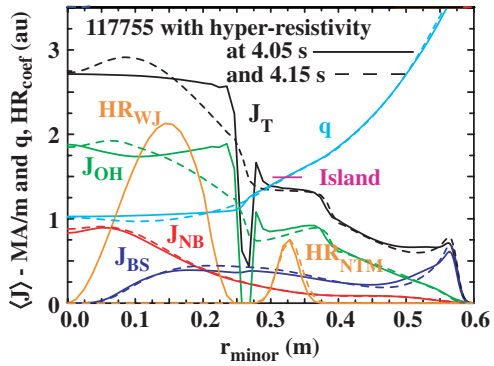

Figure 8. Flux-averaged current densities $\langle J \rangle$, q and normalized HR at 4.05 s (solid) showing current diffusion due to the WJ HR flattening of the q profile near the axis. The radial extent is limited by the presence of BFLP HR modifying the current and flux evolution in the island region. Also shown is a rebuilding of current (dotted at 4.15 s) due to flux and current diffusion that causes $q_{\min}$ to decrease with time.

of the q profile near the magnetic axis. In other simulations with an additional NTM resonant closer to the magnetic axis, e.g. a (4, 3) mode, we also were not able to obtain the flat q evolution; this needs to be explored in greater detail. Preliminary results from simulations using simultaneously active (3, 2) and (2, 2) modes were promising but led to numerical difficulties in the code that we are currently resolving. Indeed, an active area of theoretical work [8] is to determine the nature of the coupling of NTM activity to other phenomena. Thus, in the region near the magnetic axis, we use the WJ HR model [11] that is active only when q drops below 1. The WJ model also conserves helicity and adds to the effects of the BFLP model but over a different spatial region as indicated by the normalized profiles of the HR coefficient shown in figure 4.

The WJ model provides a transient correction to the q-profile near the magnetic axis, figure 8, with a negative Ohmic sheet current forming as a direct consequence of the HR model conserving helicity. For the time-slice shown, this current sheet forms at $r \sim 0.25$ m and results in a rapid change of the total current and q profiles. The current and q profiles then relax as the current density re-peaks due to a combination of noninductive current drive sources, normal flux diffusion and continuous current diffusion due to BFLP in the vicinity of the island. The form of the WJ hyper-resistivity requires the presence of a $q = 1$ surface (e.g. (1, 1) sawtooth mode). It diffuses the current so as to alter the poloidal and toroidal flux distribution inside the $q = 1$ radius and flattens the current and q profiles. To simulate the hybrid-mode characteristics, we set the WJ model to trigger when $q = 0.99$ to maintain $q_0 \sim 1$. Due to the noninductive current drive components present, $q_{\min}$ drops below 1 as the current profiles rebuild. As we show in figure 8, the NTM mode is still active in the mid-radius region and continues to modify the current and flux diffusing in the core region inside the island location. The BFLP and WJ current diffusion interact through changes in the equilibrium to alter the extent of the WJ-induced current diffusion. This coupling comes in dynamically through the equilibrium evolution that is solved at each time step in the simulation. To indicate the extent of the coupling between

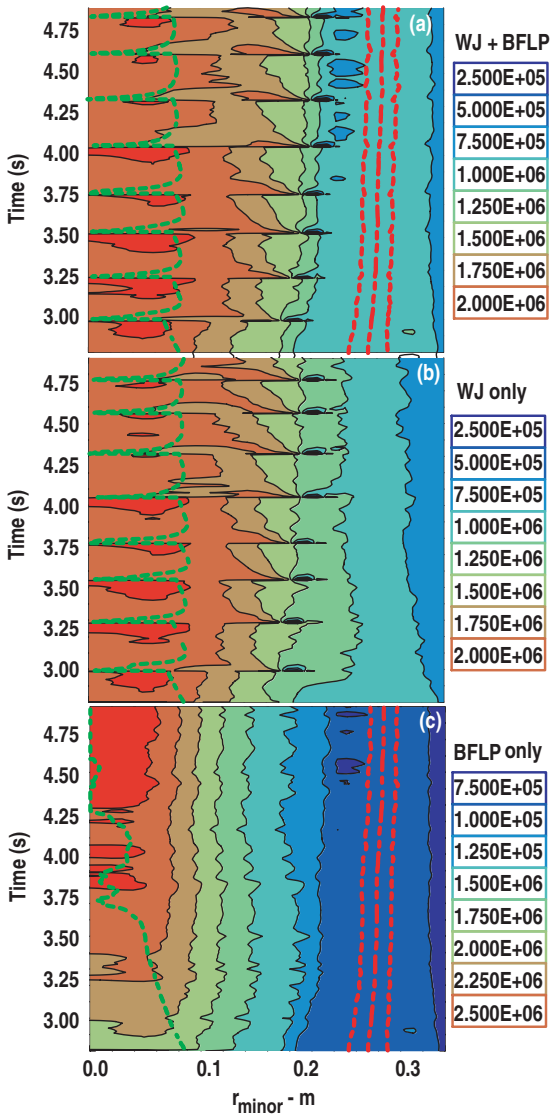

Figure 9. Contours of Ohmic current, $J_{\rm OH}$ (MA m^{-1}), for (a) both BFLP(NTM) and WJ active, (b) only WJ turned on and (c) only BFLP(NTMs) turned on. The dashed lines are the loci of $r_{\rm q\,min}$ ($r_{\rm minor} < 0.1$) and the location of the islands ($r_{\rm minor} > 0.2$, not present in (b)). Note the coupling between the BFLP and WJ models in (a) alters the contours inside the island locations with respect to (b) and (c).

these models, we show in figure 9 Ohmic current contours for three cases; both the BFLP and WJ models are active, WJ only and BFLP only, over the time interval where q_0 and $q_{\min}$ remain quasi-stationary. We observe that when the two models are simultaneously active, they both contribute to altering the contours in the region unstable to NTMs, that is, the interval $0.15\,\text{m} < r_{\rm minor} < 0.3\,\text{m}$. With BFLP present, figure 9(a), the shape of the Ohmic current contours in this region is altered with respect to those without BFLP, figure 9(b). Note that without BFLP, figure 9(b), the contour-flattening effect (near $r_{\rm minor} \sim 0.2$ m) of the WJ-induced transients extends to a larger radius and the contours in the region unstable to NTMs are narrower and move slowly inwards. Differences in the local structure of the Ohmic current-profile result in small changes to the q-profile evolution in the vicinity of the island location

although the gross structure (flattening) is ultimately set by the WJ model. Without the WJ model, figure 9(*c*), the Ohmic current contours are much narrower in radius and $r_{q\,\mathrm{min}}$ drops to zero as the q profile becomes monotonic. For the case with only BLFP active, q_0 and q_{min} continue to decrease well below unity and the q profile becomes monotonic in a manner similar to the neoclassical evolution shown in figure 6. This is further evidence that some phenomena near the magnetic axis are required to obtain the quasi-stationary evolution late in the discharge.

The WJ model is re-triggered as current density near the axis rebuilds due to flux diffusion locally re-peaking the Ohmic current. The presence of the WJ model also alters the stability of the NTM island. As is shown in figure 3, the calculated stability terms in the modified Rutherford island evolution respond to the perturbations in the equilibrium with the presence of the WJ model strongly perturbing the stabilizing Δ' term and the island width. The neoclassical term and the island radius are only very weakly modified by the presence of WJ activity. Even though the WJ model relies on a $q = 1$ resonance, q_0 and q_{min} in the quasi-stationary interval, e.g. figure 6 for $t > 3$ s, are quite consistent with the EFIT solutions and both exhibit weak negative shear q profiles ($q_0 > q_{\mathrm{min}}$) near the magnetic axis and transient excursions of $r_{q\,\mathrm{min}}$ to near zero. The simulated q_{min} tends to drop further below one due to details of the current density profile modelling in the core where the non-inductive current drive, $J_{\mathrm{BS}} + J_{\mathrm{NB}}$, is a significant fraction of the total current (30%) and of J_{OH} (50%) that results from flux diffusion effects as the current density rebuilds. As previously noted, the quasi-stationary temporal evolution of the simulated and measured MSE data near the magnetic axis, figure 7(*a*), indicates a statistical consistency in this region. As in the experiment, of particular importance in these simulations is the fact that the island evolves to a steady-state where the radial location and width remain quasi-steady in time (figures 3(*b*) and (*c*)). The purely neoclassical simulation does not establish a stationary phase in the discharge with the observed q profile characteristics. This modelling, e.g. interaction between the off-axis hyper-resistivity based on NTMs and the on-axis WJ model demonstrates that such coupling can alter the shape of the q-profile over the region of interaction. However, the relatively strong response from the WJ model tends to dominate the gross features of the q profile in the core. While the WJ model represents a magnetic reconnection for plasmas with $q < 1$, its use does reproduce quite well details of the experiment even though evidence for reconnection in these (3, 2) NTM-dominated discharges is not generally observed. In other experiments, particularly those dominated by (4, 3) mode activity, sawteeth oscillations are more often present. Future work will concentrate on analysis and modelling to explore alternative models for coupling the off-axis NTMs to phenomena near the magnetic axis (e.g. [8]) to simulate the stationary evolution phase of these hybrid mode discharges.

5. Summary and discussion

In summary, we presented analyses and modelling of HR current-profile evolution applied to hybrid-mode discharge conditions on DIII-D that appear to require some form of anomalous activity. Using HR current diffusion models that couple different regions through the equilibrium, we demonstrate that anomalous current evolution effects are capable of modelling details of the hybrid-mode current-density profile evolution and the finally achieved quasi-stationary conditions. We summarize the simulated evolution of the total current profile under the influence of the current diffusion in figure 10 to show the flattening of the current due to NTM activity and transient modification of the current that maintains $q \sim 1$. The current diffusion from the BFLP model using island parameters computed from the modified Rutherford equation in the vicinity of NTM islands continuously adjusts the evolving q-profile near the mid-radius region and modifies the profile shape during evolution to the quasi-stationary conditions. During the quasi-steady conditions, the NTM island continues to adjust the q-profile and alter the shape in the region near the island. The WJ model-induced transients dominate the q-profile (and the current profile) response when $q \sim 1$. The presence of the WJ modification to the core profile changes the stability of the NTM used to obtain the HR-coefficient in the BFLP model. While the coupling between BFLP and WJ does change the local profile characteristics near the island, the WJ model alone is sufficiently strong to flatten the q-profile. The Ohmic response to these transients in concert with the non-inductive current drive components determines the temporal response as the q-profile rebuilds. The presence of the NTM island modifies the current rebuilding process between the transients. Magnetic pitch angle data computed from a synthetic MSE diagnostic in the CORSICA simulations indicate that the

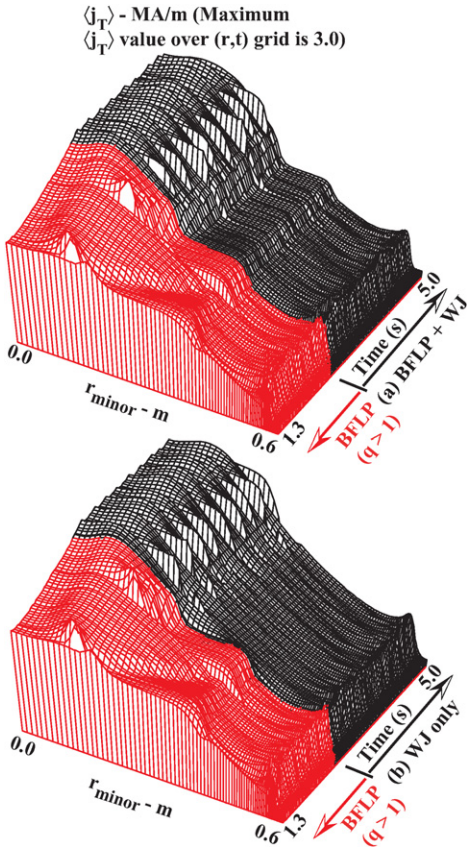

Figure 10. Simulated flux-surface-averaged total current profiles with current diffusion effects for DIII-D shot 117755.

simulated evolution is consistent with the MSE measurements on DIII-D.

Our initial intent was aimed at exploring whether the presence of a single NTM could explain the evolution of a hybrid-mode discharge. Employing the BFLP model for current diffusion, we find that a single NTM is not capable of achieving the stationary phase. We conclude that there must be some additional near-on-axis phenomena to explain this stationary q. Given the experimental observation that the presence of an off-axis NTM is necessary for achieving hybrid modes in DIII-D, we conclude that the NTM must couple to the magnetic axis region. In these simulations, the WJ model provides for gross modification of the current and q profiles near the magnetic axis and the BFLP model provides fine-scale structure changes in the vicinity of the NTM island. These fine-scale features clearly alter the dynamics of the evolution in a manner similar to both EFIT results and the MSE measurements. The gross and fine-scale features interact to mutually modify both their stability and dynamics and this in turn provides a coupling that alters the local current density. However, the rather strong and transient effect of the WJ model by itself can result in the profile flattening and the quasi-stationary behaviour late in time. This motivates us to continue to explore alternative models to represent the physical phenomena near the magnetic axis in an effort to produce a predictive model that can be used in hybrid-performance transport simulations.

Acknowledgment

The work was supported by the US Department of Energy under W-7405-ENG-48, DE-FC02-04ER54698 and DE-FG03-97ER54415.

References

[1] Luce T.C. *et al* 2001 *Nucl. Fusion* **41** 1585
[2] Staebler A. *et al* 2005 *Nucl. Fusion* **45** 617
[3] Kamada Y. *et al* 1999 *Nucl. Fusion* **39** 1845
[4] Joffrin E. *et al* 2005 *Nucl. Fusion* **45** 626
[5] Greenfield C.M. *et al* 2001 *Phys. Rev. Lett.* **86** 4544
[6] Wade M.R. *et al* 2005 *Nucl. Fusion* **45** 407
[7] Boozer A.H. 1986 *J. Plasma Phys.* **35** 133
[8] Chu M.S. *et al* 2007 *Nucl. Fusion.* **47** 434
[9] Crotinger J.A. *et al* 1997 *Lawrence Livermore National Laboratory Report* UCRL-ID-126284 available from NTIS #PB2005-102154
[10] Berk H.L., Fowler T.K., Lodestro L.L. and Pearlstein L.D. 2001 *Report* UCRL-ID-142741 http://www.osti.gov/bridge
[11] Ward D.J. and Jardin S.C. 1989 *Nucl. Fusion* **29** 905
[12] Rechester A.B. and Rosenbluth M.N. 1978 *Phys. Rev. Lett.* **40** 38
[13] Hegna C.C. 1998 *Phys. Plasmas* **5** 1767
[14] La Haye R.J. 2006 *Phys. Plasmas* **13** 055501
[15] Kotschenreuther M. *et al* 1985 *Phys. Fluids* **28** 294
[16] Casper T.A. *et al* 2004 Study of current profile evolution in presence of tearing modes in DIII-D hybrid discharges *Proc. 31st EPS Conf. (London, UK, 2004)* http://epsppd.epfl.ch/London/pdf/P2_178.pdf.
[17] Houlberg W.A., Shaing K.C., Hirshman S.P. and Zarnstorff M.C. 1997 *Phys. Plasmas* **4** 3230
[18] Pearlstein L.D., Casper T.A., Hill D.N., Lodestro L.L. and Mclean H.S. 2006 Calculation of neutral beam injection into SSPX *Proc. 33rd EPS Conf. on Plasma Physics (Rome, Italy, 2006)* http://eps2006.frascati.enea.it/papers/pdf/P5_128.pdf.
[19] Holcomb C.T., Makowski M.A., Jayakumar R.J., Allen S.L., Ellis R.M., Geer R., Behne D., Morris K.L., Seppala L.G. and Moller J.M. 2006 *Rev. Sci. Instrum.* **77** 10E506
[20] Casper T.A., Jayakumar J., Makowski M.A., and Ellis R. 2004 *Rev. Sci. Instrum.* **75** 4193
[21] Thomas D.M., Leonard A.W., Groebner R.J., Osborne T.H., Casper T.A., Snyder P.B. and Lao L.L. 2005 *Phys. Plasmas* **12** 056123